

# Parallel zippers formed by $\alpha$ -helical peptide columns in crystals of Boc-Aib-Glu(OBzl)-Leu-Aib-Ala-Leu-Aib-Ala-Lys(Z)-Aib-OMe

(double-toothed zipper/x-ray diffraction/helical peptide zipper/helix aggregation/peptide crystal structure)

ISABELLA L. KARLE\*, JUDITH L. FLIPPEN-ANDERSON\*, KUCHIBHOTLA UMA†, AND PADMANABHAN BALARAM†

\*Laboratory for the Structure of Matter, Naval Research Laboratory, Washington, DC 20375–5000; and †Molecular Biophysics Unit, Indian Institute of Science, Bangalore 560 012, India

Contributed by Isabella L. Karle, July 19, 1990

**ABSTRACT** The crystal structure of the decapeptide Boc-Aib-Glu(OBzl)-Leu-Aib-Ala-Leu-Aib-Ala-Lys(Z)-Aib-OMe (where Aib is  $\alpha$ -aminoisobutyryl, Boc is *t*-butoxycarbonyl, OBzl is benzyl ester, and Z is benzyloxycarbonyl) illustrates a parallel zipper arrangement of interacting helical peptide columns. Head-to-tail NH  $\cdots$  OC hydrogen bonding extends the  $\alpha$ -helices formed by the decapeptide into long columns in the crystal. An additional NH  $\cdots$  OC hydrogen bond in the head-to-tail region, between the extended side chains of Glu(OBzl), residue 2 in one molecule, and Lys(Z), residue 9 in another molecule, forms a “double tooth” on the side of the column. These double teeth are repeated regularly on the helical columns with spaces of six residues between them ( $\approx 10$  Å). The double teeth on a pair of parallel columns (all carbonyl groups pointed in the same direction) interdigitate in a zipper motif. All contacts in the zipper portion are of the van der Waals type. The peptide, with formula  $C_{66}H_{103}N_{11}O_{17}\cdot H_2O$ , crystallizes in space group  $P2_12_12_1$  with  $a = 10.677(4)$  Å,  $b = 16.452(6)$  Å, and  $c = 43.779(13)$  Å; overall agreement  $R = 10.2\%$  for 3527 observed reflections ( $|F_o| > 3\sigma$ ); resolution 0.9 Å.

The importance of  $\alpha$ -helix association in determining fibrous protein structures (1), in stabilizing dimeric forms of DNA-binding transcription regulatory factors, exemplified by the “leucine zipper” motif (2), and in formation of transmembrane channels by hydrophobic peptides (3) is well recognized. Crystal structure analysis of helical peptides provides a means of examining, at high resolution, modes of aggregation of  $\alpha$ -helices. Several examples of helical peptide structures in crystals have been described from our laboratories (for a review, see ref. 4), spurred largely by the goal of using rigid helical modules in *de novo* approach to synthetic protein design (5, 6). This approach has relied on the strong tendency of  $\alpha$ -aminoisobutyryl (Aib) residues to promote helical folding in peptides (7, 8). In the course of introducing polar side chains oriented on the same helix face, we synthesized the peptide Boc-Aib-Glu(OBzl)-Leu-Aib-Ala-Leu-Aib-Ala-Lys(Z)-Aib-OMe (where Boc is *t*-butoxycarbonyl, OBzl is benzyl ester, and Z is benzyloxycarbonyl), which has two bulky apolar protecting groups on the functional side chains that are seven residues apart in the sequence. In the crystal structure, intermolecular hydrogen bonds between extended glutamic acid and lysine side chains augment the head-to-tail hydrogen bonding between helical backbones. The peptide forms infinite columns with “tooth-like” extensions of the Glu(OBzl) and Lys(Z) pairs on one side. The paired side-chain extensions on a pair of peptide columns intercalate face-to-face forming a two-column entity. The assembly is in a “zipper” form with the two helix columns parallel to one another. This packing arrangement is suggestive of zipper modes of helix association different from the hypothesized “leucine zipper” for DNA

Table 1. Diffraction and crystal parameters for Boc-Aib-Glu(OBzl)-Leu-Aib-Ala-Leu-Aib-Ala-Lys(Z)-Aib-OMe

Empirical formula	$C_{66}H_{103}N_{11}O_{17}\cdot H_2O$
Crystallizing solvent	CH <sub>3</sub> OH/H <sub>2</sub> O
Color, habit	Colorless needle
Size, mm	0.2 × 0.3 × 1.0
Space group	$P2_12_12_1$
Cell parameters, Å	$a = 10.677(4)$ $b = 16.452(6)$ $c = 43.779(13)$ $\alpha = \beta = \gamma = 90^\circ$
Volume, Å <sup>3</sup>	7690(5)
Density (calc), g/cm <sup>3</sup>	1.158
Formula weight	1322.6 + 18.0
Radiation (CuK $\alpha$ , Å)	$\lambda = 1.54184$
$F(000)$	2888
Temperature	Ambient
Independent reflections	5428
Observed reflections [ $ F_o  > 3\sigma(F)$ ]	3527
Final $R$ indices, % (observed data)	$R = 10.2\%$ ; $R_w = 9.7\%$
Data/parameter ratio	4.1

binding proteins (2, 11). The structure also holds out possibilities for the synthetic design of acyclic cavities or binding sites using a helical peptide scaffold.

## EXPERIMENTAL SECTION

The decapeptide Boc-Aib-Glu(OBzl)-Leu-Aib-Ala-Leu-Aib-Ala-Lys(Z)-Aib-OMe was synthesized by conventional solution-phase procedures using a fragment-condensation approach and purified by reverse-phase HPLC (9). Crystals were grown by slow evaporation from methanol/water. X-ray diffraction data were measured on a dry crystal at room temperature with an automated four-circle diffractometer equipped with a graphite monochromator. The  $\theta/2\theta$  scan mode was used with a  $2.0^\circ + 2\theta(\alpha_1 - \alpha_2)$  scan, variable scan speeds depending upon the intensity of the reflection, and  $2\theta_{max} = 110^\circ$  (0.94-Å resolution). Three reflections, monitored after every 97 measurements, remained constant within 5% throughout the data collection. Cell parameters and diffraction data are listed in Table 1. The structure was solved by direct-phase determination using the SHELX84 package of programs (MicroVAX version of the SHELXTL system of programs, Siemens Instruments, Madison, WI). Full-matrix anisotropic least-squares refinement was performed on the C, N, and O atoms in the peptide, after which hydrogen atoms were placed in idealized positions, with C—H = 0.96 Å, and allowed to ride with the C or N atom to which each was bonded for the final cycles of refinement. The thermal factor for the

The publication costs of this article were defrayed in part by page charge payment. This article must therefore be hereby marked “advertisement” in accordance with 18 U.S.C. §1734 solely to indicate this fact.

Abbreviations: Aib,  $\alpha$ -aminoisobutyryl; Boc, *t*-butoxycarbonyl; OBzl, benzyl ester; Z, benzyloxycarbonyl.

Table 2. Atomic coordinates ( $\times 10^4$ ) and equivalent isotropic displacement coefficients ( $\text{\AA}^2 \times 10^3$ )

Atom	x	y	z	U(eq)	Atom	x	y	z	U(eq)
C(1)	9006 (14)	6849 (8)	9833 (3)	61 (1)	C $^{\alpha}$ (6)	11924 (12)	1566 (8)	8629 (3)	50 (1)
C(2)	9153 (16)	7714 (9)	9949 (4)	104 (1)	C'(6)	11855 (11)	928 (8)	8892 (3)	46 (1)
C(3)	10098 (15)	6315 (10)	9924 (4)	105 (1)	O(6)	12084 (9)	213 (5)	8833 (2)	60 (1)
C(4)	7741 (15)	6494 (10)	9914 (4)	108 (1)	C $^{\beta}$ (6)	13026 (11)	2166 (10)	8668 (4)	89 (1)
O	9026 (10)	6977 (5)	9496 (2)	66 (1)	C $^{\gamma}$ (6)*	14371 (15)	1891 (15)	8715 (8)	67 (1)
C(5)	8665 (13)	6378 (8)	9310 (4)	63 (1)	C $^{\delta 1}$ (6)*	15232 (21)	2368 (16)	8925 (8)	56 (1)
O(0)	8869 (10)	5655 (5)	9353 (2)	71 (1)	C $^{\delta 2}$ (6)*	14959 (22)	1058 (15)	8671 (12)	177 (1)
N(1)	8201 (11)	6673 (6)	9054 (3)	65 (1)	C $^{\gamma 2}$ (6)*	14123 (12)	1660 (12)	8554 (6)	167 (1)
C $^{\alpha}$ (1)	7449 (14)	6171 (8)	8838 (4)	73 (1)	C $^{\delta 3}$ (6)*	15077 (19)	2106 (17)	8359 (6)	165 (1)
C'(1)	8304 (14)	5494 (8)	8706 (3)	58 (1)	C $^{\delta 4}$ (6)*	14674 (21)	1617 (19)	8874 (6)	217 (1)
O(1)	7971 (11)	4768 (6)	8700 (2)	79 (1)	N(7)	11635 (9)	1216 (6)	9168 (2)	46 (1)
C $^{\beta 1}$ (1)	7074 (15)	6745 (9)	8578 (4)	102 (1)	C $^{\alpha}$ (7)	11638 (13)	690 (7)	9441 (3)	60 (1)
C $^{\beta 2}$ (1)	6302 (13)	5793 (9)	8996 (4)	90 (1)	C'(7)	10601 (14)	1 (8)	9388 (3)	61 (1)
N(2)	9346 (11)	5734 (6)	8576 (3)	57 (1)	O(7)	10888 (9)	-695 (5)	9472 (2)	72 (1)
C $^{\alpha}$ (2)	10123 (15)	5150 (8)	8403 (3)	69 (1)	C $^{\beta 1}$ (7)	11203 (14)	1226 (8)	9711 (3)	77 (1)
C'(2)	10838 (14)	4571 (7)	8605 (3)	58 (1)	C $^{\beta 2}$ (7)	12947 (13)	354 (8)	9496 (4)	83 (1)
O(2)	11005 (11)	3887 (6)	8531 (2)	78 (1)	N(8)	9514 (10)	235 (6)	9280 (2)	53 (1)
C $^{\beta}$ (2)	10966 (15)	5605 (9)	8190 (3)	86 (1)	C $^{\alpha}$ (8)	8534 (13)	-344 (7)	9250 (3)	57 (1)
C $^{\gamma}$ (2)	11461 (16)	5150 (10)	7959 (3)	98 (1)	C'(8)	8716 (13)	-950 (8)	8993 (3)	58 (1)
C $^{\delta}$ (2)	12002 (19)	5672 (11)	7703 (4)	133 (1)	O(8)	8083 (10)	-1590 (5)	8995 (2)	78 (1)
O $^{\epsilon 2}$ (2)	11963 (13)	6366 (7)	7669 (3)	108 (1)	C $^{\beta}$ (8)	7250 (12)	110 (9)	9210 (4)	89 (1)
O $^{\epsilon 1}$ (2)	12263 (15)	5258 (8)	7477 (4)	152 (1)	N(9)	9455 (10)	-762 (6)	8769 (2)	51 (1)
C $^{\zeta}$ (2)	12604 (18)	5688 (13)	7158 (5)	161 (1)	C $^{\alpha}$ (9)	9809 (12)	-1347 (7)	8527 (3)	52 (1)
C $^{\theta 2}$ (2)	13261 (10)	4709 (5)	6734 (2)	116 (1)	C'(9)	10715 (12)	-1962 (8)	8650 (3)	58 (1)
C $^{\iota 2}$ (2)	14267	4303	6600	168 (1)	O(9)	10612 (9)	-2679 (5)	8573 (2)	73 (1)
C $^{\kappa}$ (2)	15457	4355	6730	178 (1)	C $^{\beta}$ (9)	10322 (13)	-879 (7)	8249 (3)	58 (1)
C $^{\iota 1}$ (2)	15642	4814	6994	153 (1)	C $^{\gamma}$ (9)	10639 (14)	-1444 (9)	7990 (3)	75 (1)
C $^{\theta 1}$ (2)	14636	5221	7128	152 (1)	C $^{\delta}$ (9)	10899 (15)	-995 (9)	7704 (3)	86 (1)
C $^{\eta}$ (2)	13446	5168	6998	108 (1)	C $^{\alpha}$ (9)	11269 (16)	-1503 (11)	7426 (3)	113 (1)
N(3)	11208 (11)	4876 (6)	8877 (2)	55 (1)	N $^{\zeta}$ (9)	12503 (13)	-1960 (10)	7475 (3)	98 (1)
C $^{\alpha}$ (3)	11803 (12)	4362 (7)	9110 (3)	54 (1)	C $^{\eta}$ (9)	13559 (17)	-1598 (10)	7397 (4)	95 (1)
C'(3)	10895 (12)	3716 (8)	9228 (3)	50 (1)	O $^{\theta 2}$ (9)	13734 (12)	-919 (7)	7285 (3)	110 (1)
O(3)	11244 (8)	3003 (5)	9262 (2)	52 (1)	O $^{\theta 1}$ (9)	14553 (11)	-2083 (7)	7443 (3)	102 (1)
C $^{\beta}$ (3)	12306 (14)	4899 (9)	9368 (3)	70 (1)	C $^{\iota}$ (9)	15791 (16)	-1751 (10)	7402 (6)	141 (1)
C $^{\gamma}$ (3)	12961 (15)	4451 (10)	9633 (4)	88 (1)	C $^{\lambda 1}$ (9)	17637 (10)	-2396 (6)	7206 (2)	161 (1)
C $^{\delta 1}$ (3)	14062 (16)	3950 (12)	9525 (5)	143 (1)	C $^{\mu 1}$ (9)	18578	-2984	7204	145 (1)
C $^{\delta 2}$ (3)	13419 (18)	5055 (11)	9857 (4)	209 (1)	C $^{\nu}$ (9)	18552	-3618	7416	154 (1)
N(4)	9731 (10)	3947 (6)	9293 (3)	50 (1)	C $^{\mu 2}$ (9)	17585	-3663	7629	196 (1)
C $^{\alpha}$ (4)	8771 (14)	3399 (8)	9397 (3)	60 (1)	C $^{\lambda 2}$ (9)	16645	-3075	7632	223 (1)
C'(4)	8704 (12)	2668 (8)	9157 (3)	52 (1)	C $^{\kappa}$ (9)	16670	-2441	7420	119 (1)
O(4)	8627 (10)	1961 (5)	9238 (2)	62 (1)	N(10)	11623 (10)	-1717 (6)	8834 (2)	55 (1)
C $^{\beta 2}$ (4)	9034 (15)	3051 (9)	9719 (3)	80 (1)	C $^{\alpha}$ (10)	12561 (12)	-2258 (7)	8962 (3)	51 (1)
C $^{\beta 1}$ (4)	7455 (13)	3797 (8)	9403 (4)	72 (1)	C'(10)	13081 (13)	-2850 (9)	8714 (3)	68 (1)
N(5)	8656 (10)	2896 (6)	8867 (2)	48 (1)	O(10)	13280 (11)	-3552 (6)	8766 (3)	96 (1)
C $^{\alpha}$ (5)	8512 (12)	2312 (8)	8623 (3)	48 (1)	C $^{\beta 2}$ (10)	11936 (14)	-2749 (8)	9218 (3)	82 (1)
C'(5)	9666 (13)	1731 (7)	8607 (3)	51 (1)	C $^{\beta 1}$ (10)	13661 (13)	-1755 (8)	9089 (3)	74 (1)
O(5)	9479 (9)	1015 (5)	8547 (2)	63 (1)	O(11)	13432 (9)	-2422 (6)	8474 (2)	74 (1)
C $^{\beta}$ (5)	8306 (13)	2739 (8)	8335 (3)	69 (1)	C(11)	13943 (15)	-2891 (10)	8231 (3)	108 (1)
N(6)	10768 (11)	2052 (6)	8641 (2)	49 (1)	W(1)	15023 (18)	-123 (13)	6760 (5)	282 (1)

Numbers in parentheses are SD. Equivalent isotropic  $U [U(\text{eq})]$  is one-third of the trace of the orthogonalized  $U_{ij}$  tensor.

\*Disordered leucyl side chain.

hydrogen atoms was fixed at  $U_{\text{iso}} = 0.125$ . The phenyl moieties in the two blocking groups OBzl and Z have large thermal parameters that made least-squares refinement difficult. Accordingly, both phenyl groups were constrained to be regular hexagons with C—C distances of 1.395 Å, although the position and orientation of each hexagon and the anisotropic thermal values for each atom in the hexagons were subjected to least-squares refinement. Furthermore, the C $^{\gamma}$  and C $^{\delta}$  atoms in the side-chain of Leu-6 are disordered. Difference maps and further cycles of refinement were used to approximate two positions for the side chains at 70% and 30% occupancy. In this case also, the C—C atoms in the side chains were constrained to be near 1.52 Å. The above constraints and approximations to describe disorder account for the relatively large factor of 10.2%.

Fractional coordinates for the C, N, and O atoms are listed in Table 2. Bond lengths and bond angles (estimated SD,  $\approx 0.02$  Å for bonds and  $1.2^\circ$  for angles) do not show significant or systematic differences from expected values. $^{\ddagger}$

## RESULTS

**The Peptide Helix.** The decapeptide crystallizes in the form of an  $\alpha$ -helix with seven intrahelical hydrogen bonds of the

$^{\ddagger}$ Supplementary material consisting of bond lengths and angles, anisotropic thermal factors, and coordinates for hydrogen atoms is being deposited with the Cambridge Structural Data Base, University Chemical Laboratory, Lensfield Road, Cambridge CB2 1EW, United Kingdom. Lists of observed and calculated structure factors are available from I.L.K. and J.L.F.-A.

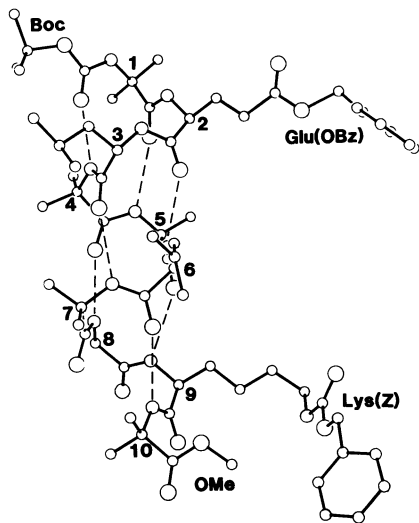


FIG. 1.  $\alpha$ -Helix conformation of Boc-Aib-Glu(OBzl)-Leu-Aib-Ala-Leu-Aib-Ala-Lys(Z)-Aib-OMe. The diagram was drawn using the experimentally determined coordinates from the crystal structure analysis. Hydrogen bonds of the 5  $\rightarrow$  1 type are indicated by dashed lines. The C $^{\alpha}$  atoms are labeled 1–10.

5  $\rightarrow$  1 type, shown in Fig. 1. Conformational angles for the backbone and side chains are listed in Table 3. The peptide helices repeat along the *b* axis by translation. Head-to-tail hydrogen bonds, formed between N(1)H  $\cdots$  O(8) and N(2)H  $\cdots$  O(9), effectively continue the helix throughout the crystal along the *b* axis. The N(3)H moiety does not participate in any hydrogen bonding. The N(3)  $\cdots$  O(10) distance is 3.49 Å and a N(3)  $\cdots$  O(10) head-to-tail hydrogen bond is not possible because of a helix reversal at C $^{\alpha}$ (10) for Aib-10. See Table 4 for listing of hydrogen bond parameters.

An additional hydrogen bond is formed in the head-to-tail region that involves the side chains of residues Glu(OBzl)-2 and Lys(Z)-9, N $^{\zeta}$ (9)  $\cdots$  O $^{\epsilon 2}$ (2), between molecules stacked over each other, as seen in Fig. 2.

**Toothed Column Formation.** The three direct NH  $\cdots$  OC hydrogen bonds in the head-to-tail region maintain a column of backbone helices from individual peptide molecules that approximates very closely an  $\alpha$ -helix of many turns. Fig. 3, a grid representing an ideal  $\alpha$ -helix (that has been flattened into two dimensions by splitting the helix lengthwise) is used to display the column assembly for the present structure. The

long dashed lines represent the boundaries (head-to-tail regions) between peptides. The short dashed lines represent 5  $\rightarrow$  1 and head-to-tail hydrogen bonds and the heavy lines represent the side chains linked by NH  $\cdots$  OC hydrogen bonds. In the crystal of the peptide, there is an exact repeat in the vertical (*b* axis) direction, whereas, in the  $\alpha$ -helix representation in Fig. 3, there is a slight tilt from the vertical of an imaginary line passing through repeating parts of the peptide molecules [see the glutamic acid (E) residues, e.g.].

The C $^{\alpha}$  atoms for Glu(OBzl)-2 and Lys(Z)-9, separated by seven residues, occur almost directly over each other in the helix backbone as in an ideal  $\alpha$ -helix. The C $^{\alpha}$ (2)  $\cdots$  C $^{\alpha}$ (9) distance is 10.7 Å and, in the extended side chains, the O $^{\epsilon 1}$ (2)  $\cdots$  C $^{\delta}$ (9) separation is 10.4 Å. The “head-to-tail” N $^{\zeta}$ (9)  $\cdots$  O $^{\epsilon 2}$ (2) hydrogen bond ties the two long extended side chains from neighboring molecules into one unit. As a result there is effectively a continuous  $\alpha$ -helix with equally spaced protruding teeth on one side composed of two side chains from neighboring molecules. A segment of such a toothed column is shown by the two open molecules in Fig. 2.

**Zipper Assembly.** The teeth of one helix column interdigitate with the teeth of another column, as is illustrated in Fig. 2 by the open and solid molecules. Only one solid molecule is shown. The interdigitation is not with single side chains but with pairs of side chains from each column. Furthermore, the helix directions of the two columns are parallel rather than antiparallel. In the crystal, the interdigitating columns are related by a twofold screw operation. Contacts between atoms in the interdigitating side chains are only of the van der Waals type,  $\approx$ 3.85–4.10 Å.

The teeth on one side of the zipper are indicated in Fig. 3 by the one-letter symbols E and K that are joined by a heavy line. The helix scaffold with protruding double teeth is shown in Fig. 4 in a space-filling representation.

**Crystal Packing.** The zippered pairs of helices pack in a herring-bone pattern, as shown in Fig. 5, where the view is directed into the helices (down the *b* axis). The top of the helices is labeled N (N terminus) or C (C terminus). Along the *c* axis, double sheets of helices, all pointed in one direction, alternate with double sheets that point in the opposite direction.

A single water molecule cocrystallizes with each peptide molecule. It participates in only one hydrogen bond, with the carbonyl in the side chain of Lys(Z), W(1)  $\cdots$  O $^{\theta 2}$ (9) (Fig. 2). The next nearest neighbor of W(1) is O(1) at a distance of 3.78 Å.

Table 3. Torsion angles

Residue	Torsion angle, degrees								
	$\phi$	$\psi$	$\omega$	$\chi^1$	$\chi^2$	$\chi^3$	$\chi^4$	$\chi^5$	$\chi^6$
Aib-1	-65*	-55	-171						
Glu-2 <sup>†</sup>	-74	-32	174	-162	164	-170	168	151	-75, 110
Leu-3	-65	-45	178	180	58, 178				
Aib-4	-53	-48	-176						
Ala-5	-64	-42	180						
Leu-6	-61	-53	-175	171	14 <sup>‡</sup> , -144				
Aib-7	-59	-45	-176						
Ala-8	-72	-22	173						
Lys-9 <sup>§</sup>	-73	-41	-179	-177	169	178	-61	-90	-178
Aib-10	+45	+51 <sup>¶</sup>	-179 <sup>  </sup>						

Torsion angles for rotation about bonds of the peptide backbone ( $\phi$ ,  $\psi$ , and  $\omega$ ) and about bonds of the amino acid side chains ( $\chi^n$ ) are described in ref. 10. Estimated standard deviations were  $\approx$ 1.5°.

\*C $^{\alpha}$ (0), N(1), C $^{\alpha}$ (1), C'(1).

<sup>†</sup>OBzl, benzyl ester.

<sup>‡</sup>Disordered side chain, 70% occupancy;  $\chi^1$  and  $\chi^2$  also -163°, (140°, -112°) for 30% occupancy.

<sup>§</sup>Z, benzyloxycarbonyl;  $\chi^7$ ,  $\chi^8$ ,  $\chi^9$  have values -173°, -171°, and (139°, -44°), respectively.

<sup>¶</sup>N(10), C $^{\alpha}$ (10), C'(10), O(OMe).

<sup>||</sup>C $^{\alpha}$ (10), C'(10), O(OMe), C(OMe).

Table 4. Hydrogen bonds

Type	Donor	Acceptor	N ··· O, Å	H ··· O*, Å	Angle, degrees (C=O ··· N)
Head-to-tail	N(1)	O(8) <sup>†</sup>	2.872	1.96	144
	N(2)	O(9) <sup>†</sup>	2.939	2.01	153
	N(3)				
5 → 1	N(4)	O(0)	2.970	2.04	164
	N(5)	O(1)	3.248	2.35	147
	N(6)	O(2)	3.069	2.18	152
	N(7)	O(3)	2.999	2.04	162
	N(8)	O(4)	3.000	2.09	154
	N(9)	O(5)	3.082	2.26	148
	N(10)	O(6)	3.212	2.30	156
Side chain/side chain	N <sup>‡</sup> (9)	O <sup>‡2</sup> (2)	2.891	2.01	164
Water/side chain	W(1)	O <sup>‡1</sup> (9)	2.986		

\*H atoms were placed in idealized positions with the N—H distance equal to 0.96 Å.

<sup>†</sup>Symmetry equivalents  $x, 1 + y, z$  to coordinates listed in Table 2.

<sup>‡</sup>Symmetry equivalents  $x, -1 + y, z$  to coordinates listed in Table 2. Atoms N(3)H, O(7), and O(10) do not participate in any hydrogen bonding.

## DISCUSSION

The present crystal structure reveals an extraordinarily well-packed parallel zipper arrangement between two columns of helical peptide molecules. Each tooth of the zipper consists of a pair of residues that repeats after seven residues. If we refer to Fig. 3, the repeating pairs of teeth occur at positions (9, 13), (20, 24), (31, 35), etc. Furthermore, each double-sized tooth from a neighboring parallel peptide interdigitates into the 7-residue interval between teeth. The teeth are particu-

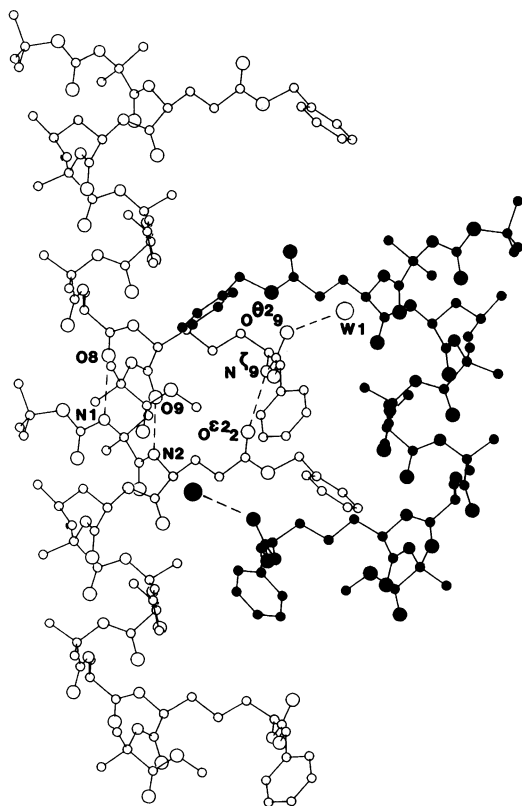


FIG. 2. Assembly of peptides into a continuous column by head-to-tail hydrogen bonding between helix backbones, N(1) ··· O(8) and N(2) ··· O(9), and between side chains, N<sup>‡</sup>(9) ··· O<sup>‡2</sup>(2) (see the open molecules). The solid molecule, representative of another continuous column related to the open column by a vertical twofold screw axis, does not have any hydrogen bonds in common with the open column. Interdigitation of side chains on residues 2 and 9 takes place by pairs, two open, two solid, etc. in a zipper motif.

larly long (especially since blocking groups are attached to the glutamic acid and lysine side chains that compose each tooth) in comparison to neighboring side chains. The heptad repetition of bulky projections on a helical backbone is reminiscent of the hypothesized leucine-zipper arrangement suggested for a specific class of DNA binding proteins (2, 11). Although the leucine-zipper motif has not been crystallographically characterized so far, the weight of available evidence, in solution, suggests that the interacting  $\alpha$ -helices associate in a parallel coiled-coil arrangement (12). Heptad repeats of apolar residues are also found in fibrous coiled-coil structures, where efficient meshing of the interacting polypeptides occurs by bending of the helical chains, which then wind around one another with a net supercoil (1). Such arrangements lead to optimum interlocking of projecting side chains, a feature linked to the heptad sequence repeats of appropriate residues (13). Crystal structures of several leucine-rich  $\alpha$ -helical peptides, carried out in these laboratories (6, 14–16), have provided an opportunity to examine the role of Leu–Leu interactions in helix packing. There have been no

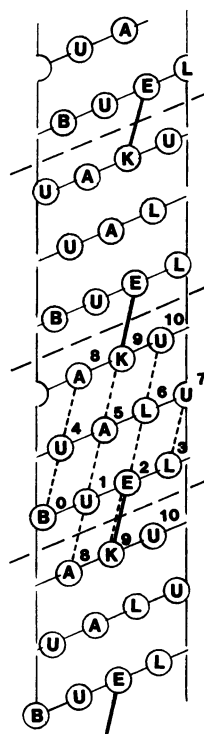


FIG. 3. Two-dimensional grid representing an ideal  $\alpha$ -helix is used to display a column of helices from the present structure that is formed by repeating molecules along the  $b$  axis. The long dashes represent boundaries between individual peptides, the short dashes represent hydrogen bonds of the 5 → 1 type and head-to-tail, and the heavy line is the hydrogen bond link between side chains in Glu(OBzl)-2 and Lys(Z)-9. The one letter code for residues is used in this diagram. B, Boc.

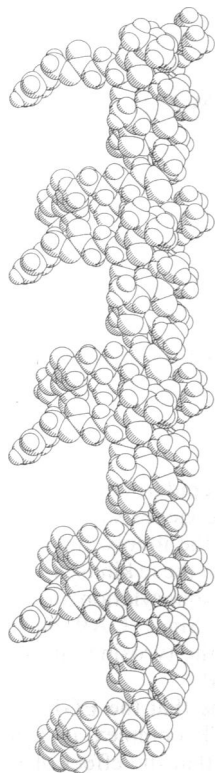


FIG. 4. Space-filling representation of the double-toothed  $\alpha$ -helix column in the orientation of the solid molecules in Fig. 2. The figure was drawn using the coordinates obtained from the crystal structure analysis.

particular Leu–Leu attractions except in two crystals. In the crystal of Boc-Aib-Leu-Aib-Aib-Leu-Leu-Leu-Aib-Leu-Aib-OMe, where Leu-2, Leu-6, and Leu-9 occur on one side of the helix, the C $^{\beta}$  atoms of the leucine residues butt against each other in neighboring parallel molecules (unpublished data). In the crystals of Boc-(Aib-Ala-Leu) $_3$ -Aib-OMe, a hydrophobic peptide that has been rendered amphipathic by the entry of a water molecule into the helix, Leu-3 and Leu-6 are adjacent to each other on the other side of the helix. Since there is not enough space between adjacent leucyl side chains for others to penetrate in the same “plane,” the interdigitating leucyl side chains from neighboring adjacent molecules (anti-parallel) are offset (16). In the present structure, the unusually long projecting side chain permits efficient packing, leading to a zipper structure without any helix axis bending or coiling.

A particularly interesting feature is the approximately “U” shaped nature of the molecule, with the helix backbone forming the base and the side chains, the arms. The result is the development of a large cavity or binding side, which then accommodates the bulky protecting groups of two molecules in an adjacent column that are vertically offset. Clearly, in this structure the presence of both aromatic rings and polar functions like ester and urethane bonds can provide a reasonably versatile set of liganding groups. This suggests several possibilities for synthetic elaboration of large acyclic cavities, opening promising areas of host–guest chemistry.

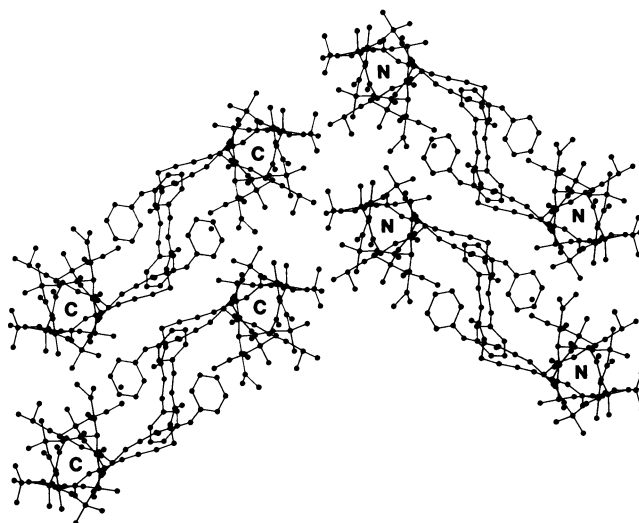


FIG. 5. Crystal packing of the zippered (interdigitated) pairs of helices with a view into the helices (along the  $b$  axis). The N or C termini at the top are labeled N or C. Axial directions for the cell are  $a$  (vertical) and  $c$  (horizontal).

This research was supported in part by National Institutes of Health Grant GM30902, in part by the Office of Naval Research, and in part by a grant from the Department of Science and Technology, India.

1. Cohen, C. & Parry, D. A. D. (1990) *Proteins Struct. Funct. Genet.* **7**, 1–15.
2. Vinson, C. R., Sigler, P. B. & McKnight, S. L. (1989) *Science* **246**, 911–916.
3. Mathew, M. K. & Balam, P. (1983) *Mol. Cell. Biochem.* **50**, 47–64.
4. Karle, I. L. & Balam, P. (1990) *Biochemistry* **29**, 6747–6756.
5. Karle, I. L., Flippen-Anderson, J. L., Uma, K. & Balam, P. (1989) *Biochemistry* **28**, 6696–6701.
6. Karle, I. L., Flippen-Anderson, J. L., Uma, K., Sukumar, M. & Balam, P. (1990) *J. Am. Chem. Soc.*, in press.
7. Prasad, B. V. V. & Balam, P. (1984) *CRC Crit. Rev. Biochem.* **16**, 307–348.
8. Uma, K. & Balam, P. (1989) *Indian J. Chem.* **28**, 705–710.
9. Balam, H., Sukumar, M. & Balam, P. (1986) *Biopolymers* **25**, 2209–2223.
10. IUPAC-IUB Commission on Biochemical Nomenclature (1970) *Biochemistry* **9**, 3471–3479.
11. Landschulz, W. H., Johnson, P. F. & McKnight, S. L. (1988) *Science* **240**, 1759–1764.
12. O’Shea, E. K., Rutkowski, R. & Kim, P. S. (1989) *Science* **243**, 538–542.
13. Crick, F. H. C. (1953) *Acta Crystallogr.* **6**, 689–697.
14. Karle, I. L., Flippen-Anderson, J. L., Uma, K. & Balam, P. (1990) *Biopolymers* **29**, 1835–1845.
15. Karle, I. L., Flippen-Anderson, J. L., Uma, K. & Balam, P. (1990) *Curr. Science*, in press.
16. Karle, I. L., Flippen-Anderson, J. L., Uma, K. & Balam, P. (1988) *Proc. Natl. Acad. Sci. USA* **85**, 299–303.